Discontinuous Phase Transitions in Nonlocal Schloegl Models for Autocatalysis: Loss and Reemergence of a Nonequilibrium Gibbs Phase Rule

Da-Jiang Liu, Chi-Jen Wang, and James W. Evans

Phys. Rev. Lett. **121**, 120603 — Published 21 September 2018

DOI: 10.1103/PhysRevLett.121.120603

Discontinuous phase transitions in non-local Schloegl models for autocatalysis: Loss and reemergence of a non-equilibrium Gibbs phase rule

Da-Jiang Liu,[1] Chi-Jen Wang[2] and James W. Evans[1,3,4]

[1]Ames Laboratory – USDOE, Iowa State University, Ames, Iowa 50011, USA
[2]Department of Mathematics, National Chung Cheng University, Chiayi 62102, Taiwan
[3]Department of Mathematics, Iowa State University, Ames, Iowa 50011, USA
[4]Department of Physics and Astronomy, Iowa State University, Ames, Iowa 50011, USA

Abstract

We consider Schloegl models (or contact processes) where particles on a square grid annihilate at rate p, and are created at rate $k_n = \frac{n(n-1)}{N(N-1)}$ at empty sites with n particles in a neighborhood, Ω_N, of size N. Simulation reveals a discontinuous transition between populated and vacuum states, but equistable $p=p_{eq}$ determined by stationarity of planar interfaces between these states depend on interface orientation and Ω_N. Behavior for large Ω_N follows from continuum equations. These also depend on interface orientation and Ω_N-shape, but a unique p_{eq}=0.211376… emerges imposing a Gibbs phase rule.

Text

Basic open questions remain regarding phase transitions between steady-states in statistical mechanical models of non-equilibrium systems where a free energy framework is not available to aid analysis [1-5]. For discontinuous transitions with a single control parameter, p, the Gibbs phase rule in equilibrium systems requires that these transitions occur at a unique $p = p_{eq}$ where the two phases coexist with equal chemical potentials [6]. For non-equilibrium systems, phase coexistence or equistability is usually determined by stationarity of a planar interface separating the two phases [7,8], a criterion also applicable to equilibrium systems. However, for non-equilibrium systems, phase coexistence can occur over a finite range of control parameter, p (so-called generic two-phase coexistence, 2PC) [9-14]. This feature can be manifested by a dependence of p_{eq} on interface orientation. In a regime of generic 2PC, both states are in some sense stable against perturbation by the other state. Such behavior is manifested, e.g., in Toom's model [9-11], pinned interface models [12], and certain contact processes [13,14]. In addition to elucidating poorly understood generic 2PC, related challenges remain for characterization of metastability and associated nucleation phenomena [15-18].

To advance fundamental understanding of these issues, it is desirable to construct suitable single-component stochastic lattice-gas models with simple "symmetric rules" (avoiding an asymmetry in Toom's rules and the complexity of heterogeneous interface pinning models or of multi-component models). Furthermore, the models are naturally constructed to exhibit mean-field (MF) analysis bistability of steady-states. MF bistability is a ubiquitous phenomena in both equilibrium systems (e.g., van der Waals equation of state) and in diverse non-equilibrium systems (describing catalysis, spatial epidemics, population dynamics, etc.) [19,20]. It can signal

the presence of a discontinuous transition in the stochastic model where fluctuations and correlations generally preclude exact analysis. We will explore a suitably crafted class of models motivated by Schloegl's second model for autocatalysis [13,14,17,20-24] where particles reside at the sites of a square lattice. Particles spontaneously annihilate at rate p, and are created autocatalytically at empty sites if there are $n \geq 2$ particles within a prescribed neighborhood of that site. These models are equivalent to spatial contact processes with threshold 2 describing the spread of epidemics [13,14,25-31]. In this application, empty (filled) sites in the Schloegl model are reassigned as healthy (infected) sites. Then, infected sites recover at rate *p*, and healthy sites can become infected given two or more nearby infected individuals. Such contact processes are also adopted to describe, e.g., the spread of information.

Often the neighborhood influencing particle creation (or infection) includes just four nearest-neighbor (NN) sites. Studies of these models revealed a discontinuous phase transition exhibiting generic 2PC [13,14,17]. However, this is not broadly recognized or accepted [30,31], perhaps since a prominent study by Grassberger [22] of one realization of Schloegl's second model revealed a continuous transition (but this does not imply the same is true of other realizations). Here, we allow the possibility of general neighborhoods, Ω_N, of N sites, and judiciously select creation rates $k_n = \frac{\binom{N-2}{n-2}}{\binom{N}{n}} = \frac{\binom{n}{2}}{\binom{N}{2}} = \frac{n(n-1)}{N(N-1)}$ to ensure that all models share the same MF kinetics (see below). Our extension to general "non-local" neighborhoods reflects a strategy used for elucidation of critical phenomena in equilibrium [32,33] and non-equilibrium [34,35] models, and connects with classic non-local continuum contact processes for epidemic or information spread with long-range infection or communication [36]. Furthermore, construction of this general class of models allows us to address a postulate by Grinstein and coworkers [37] that model discreteness is not intrinsic to generic 2PC, i.e., if a discrete model incorporates features inducing generic 2PC, then the same should hold for the analogous continuum model. We find that this is not the case for our models.

In this Letter, first for our new appropriately crafted class of non-local Schloegl models, we develop an exact master equation based formulation describing model behavior importantly including heterogeneous states. Next, we present results from suitably tailored Kinetic Monte Carlo (KMC) simulations within a constant-concentration ensemble precisely assessing model behavior both for small Ω_N where 2PC is revealed, and for large Ω_N where surprisingly a unique and universal p_{eq} emerges. For deeper understanding of the latter, we provide an analytic treatment of interface propagation for large Ω_N in terms of continuum integro-differential equations (IDEs) which are rigorously derived from the above exact heterogeneous master equations. While stationary front solutions for continuum reaction-diffusion equations (RDEs) can often be analyzed by direct mapping onto a Hamiltonian problem [20], this is not the case for IDEs. Nonetheless, exact analysis of the IDE is achieved by mapping onto an infinite-dimensional dissipative dynamical system. This integrated combination of tailored KMC simulation and novel analytic analysis enables a significant advance in the current

limited understanding of subtle generic 2PC phenomena and of the applicability or otherwise of Gibbs type phase rules for non-equilibrium systems.

For spatially homogeneous states, the overall fraction or concentration, $C=C(t)$, of populated sites in our models satisfies

$$d/dt\ C \equiv R(C, p) = -pC + K_{tot}, \quad (1)$$

for total particle creation rate per site $K_{tot} = \sum_{2\le n\le N} k_n P_n (1-C)$. Here P_n is the probability of exactly n populated sites in Ω_N which reflects non-trivial spatial correlations. If p is not too large, there will exist an populated steady-state with $C=C_{act}(p)>0$, and $C(t)\to C_{act}(p)$ for sufficiently high $C(0)$. One finds that $C_{act}(p)\approx 1-p$, as $p\to 0$, since $K_{tot}(p) \approx k_N(1-p) = 1-p$. For sufficiently large p, annihilation overwhelms particle creation, and $C(t)\to C_{vac}(p) \equiv 0$, the absorbing vacuum steady-state. This absorbing state exists for all $p > 0$. Finally, we note that a MF treatment neglecting spatial correlations in site population implies that $P_n = \binom{N}{n} C^n (1-C)^{N-n}$. Consequently, the MF K_{tot} and $R(C)$ are independent of Ω_N, and given by

$$K_{tot}(MF) = (1-C)C^2, \text{ and } R_{MF}(C, p) = -pC + (1-C)C^2. \quad (2)$$

The MF steady states are given by $C_{\pm}(p) = \frac{1}{2} \pm \frac{1}{2}(1-4p)^{1/2}$, for $0 \le p \le \frac{1}{4}$, and $C=0$ (the vacuum). C_+ corresponds to the stable populated state, and C_- to an unstable state. As an aside, we remark that the same MF kinetics applies for Durrett's $N=4$ model where Ω_4 includes NN sites and creation rates satisfy $k = m/4$ where m is the number of diagonal NN populated pairs in Ω_4 [13,25].

Analysis of spatially heterogeneous states, and specifically the propagation of interfaces between populated and vacuum steady states, is central to assessment of equistability. Thus, we develop an exact heterogeneous version [24,38,39] of (1). Let $C_{i,j} = P[x_{i,j}]$ denote the ensemble-averaged probability that site (i,j) is occupied (x), and $P[o_{i,j}]$ the probability that site (i,j) is empty (o), so that $P[x_{i,j}] + P[o_{i,j}] = 1$. Also, let $P[o_{i,j} - x_{k,l} - x_{m,n}]$ denote the probability that (i,j) is empty and both (k,l) and (m,n) are occupied, etc. Then, one has that

$$d/dt\ C_{i,j} = -p\ C_{i,j} + K_{tot}(i,j), \quad (3)$$

where $K_{tot}(i,j)$ denotes the total rate of particle creation at site (i,j). $K_{tot}(i,j)$ involves a sum over contributions for each possible configuration of the neighborhood $\Omega_N(i,j)$ of empty site (i,j) with $n \ge 2$ populated sites associated with rate $k_n = \frac{\binom{n}{2}}{\binom{N}{2}}$. Each such contribution can be partitioned into $\binom{n}{2}$ equal contributions of $1/\binom{N}{2}$ times the relevant configuration probability for each of the $\binom{n}{2}$ pairs of populated sites. Combining all contributions associated with a specific populated pair, $K_{tot}(i,j)$ reduces exactly to a sum over 3-site probabilities with (i,j) is empty and the specific pair populated,

$$K_{tot}(i,j) = \sum_{(i',j')\neq(i'',j'')\in\Omega_N} P[o_{i,j} - x_{i+i',j+j'} - x_{i+i'',j+j''}] \,/\binom{N}{2}, \qquad (4)$$

The sum has $\binom{N}{2}$ terms avoiding double-counting pairs of sites in Ω_N. This exact reduction from (N+1)-site to 3-site probabilities follows from our special choice of k_n. Applying (4) for uniform states immediately recovers the MF result (2) after factorizing the 3-site probability. More significantly, (4) will facilitate analytic treatment of behavior for large Ω_N, as described below.

Next, we assess model behavior from KMC simulation. For discontinuous transitions, constant-concentration (CC) simulation [13,40,41] is particularly efficient. One selects a target concentration, C_t, and by default initially populates sites randomly with $C \approx C_t$. Then, one picks a site at random, and attempts to create (annihilate) a particle at that site if the current concentration satisfies $C<C_t$ ($C\geq C_t$). Tracking relative creation and annihilation rates produces a $p=p_t$ corresponding to $C=C_t$. KMC results for steady-state $C(p)$ versus p are shown in Fig.1 mainly for square Ω_N. A discontinuous transition at $p=p_{eq}(N)$ occurs for all Ω_N, where $p_{eq}(N) \approx p_{eq}(\infty) - c/N$, for large N, for both the square and circular Ω_N, and where $p_{eq}(\infty)\approx 0.2113(1)$ appears independent of neighborhood shape. See Fig.2. Simulated configurations for $C_t \approx 0.5$ directly reveal phase separation. Convergence to MF behavior is evident for large N, as elucidated below.

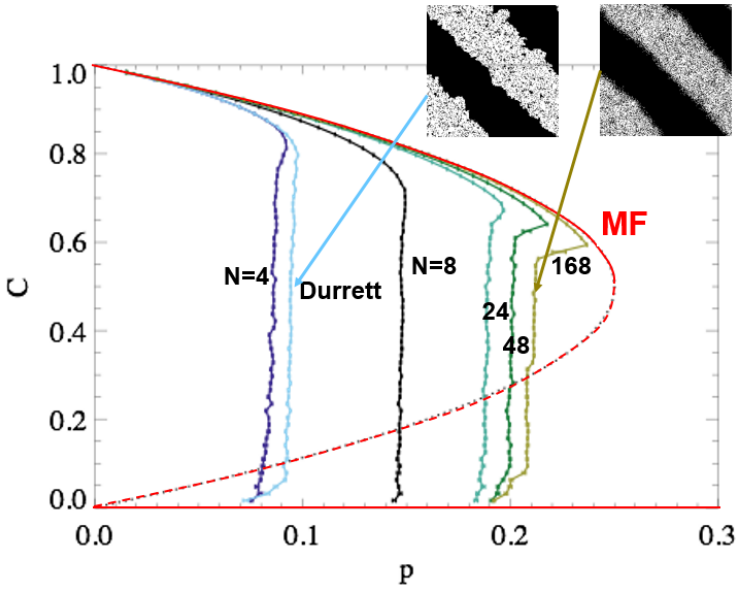

FIG.1. Steady-state C versus p for square Ω_N for $N=L^2-1$ with $L\geq 3$, and for $N=4$ from KMC; $C=0$ above the transition. MF behavior is also shown. Inset: $S=1$ strip geometries for $N=4,128$.

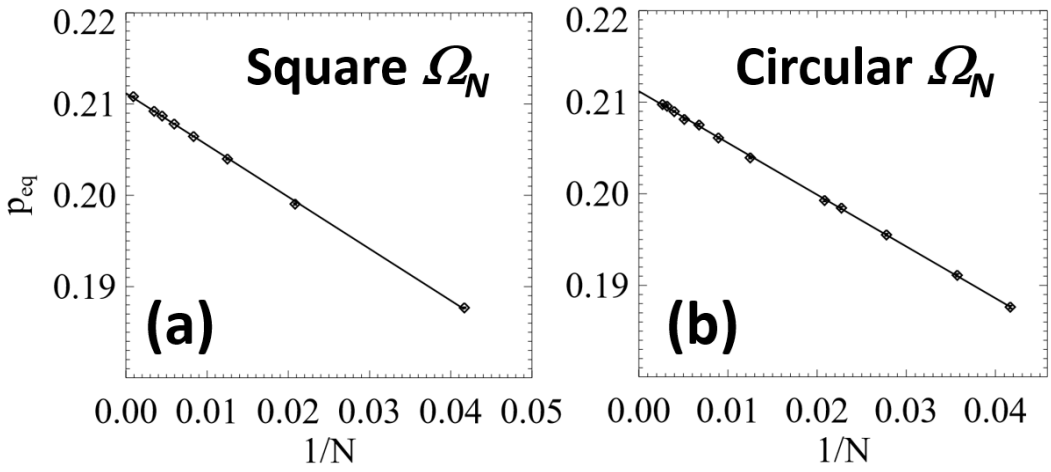

FIG. 2. $p_{eq}(N)$ for (a) square and (b) circular Ω_N.

Refinement to the above basic CC simulation analysis is needed to assess any orientation-dependence of equistability. Here, one starts with a strip of populated sites with selected orientation or slope, S, which is preserved provided the simulation maintains a strip geometry. Results of such simulations reveal an unambiguous variation of $p_{eq}(S)$ with S for N=4 with NN sites (a distance $r = a$ from the empty site for lattice constant a), N=8 with 4NN sites ($r = \sqrt{5}a$), N=8 with NN & 3NN sites ($r = a, 2a$), and N=12 (with $r = a, 2a, 3a$). See Table I. For N = 8 with NN & 2NN sites ($r = a, \sqrt{2}a$) and for N>8, it is difficult to quantify any weak S-dependence of $p_{eq}(S)$, although plausibly this persists. In the simulations of Fig.1 with random initial conditions, p_{eq} reflects an average over S of $p_{eq}(S)$.

Table I: $p_{eq}(S)$ versus S from CC simulations (1024x1024 cell with PBC for 10^5 MCS) with strip geometries for indicated Ω_N. Uncertainties from 45 simulations for 5 different C_t from 0.62-0.70. Less reliable results for N=4 with S=0 are omitted (cf. [13,24]).

Slope S	N=4 (r = a)	N=8 ($\sqrt{5}$a)	N=8 (a,2a)	N=8 (a,$\sqrt{2}$a)	N=12(a,2a,3a)
0	-------	0.151121(2)	0.147948(13)	0.146807(3)	0.168721(12)
1/6	0.080480(8)	0.151111(1)	0.147939(6)	0.146802(2)	0.168766(9)
1/5	0.081151(9)	0.151109(1)	0.147957(6)	0.146808(1)	0.168771(7)
1/4	0.081978(8)	0.151100(1)	0.147976(7)	0.146808(1)	0.168793(8)
1/3	0.082974(10)	0.151090(1)	0.148004(6)	0.146806(1)	0.168828(7)
1/2	0.084134(13)	0.151070(1)	0.148086(9)	0.146807(2)	0.168899(10)
1	0.084941(40)	0.151037(2)	0.148134(10)	0.146806(2)	0.169000(11)

Henceforth, we focus on providing insight into limiting behavior for large compact neighborhoods as $N\to\infty$. The distribution, P_n, of the number n of populated sites within Ω_N becomes narrowly distributed about the mean $n = N\cdot C$, so that $K_{tot} = \sum_{2\le n\le N} k_n P_n(1\text{-}C) \approx k_{n=NC}(1\text{-}C) \to (1\text{-}C)C^2$, as $N \to \infty$ explaining the recovery of MF kinetics. However, our focus is on heterogeneous states. Thus, we consider a coarse-grained spatially continuous description of the concentration $C(\underline{x}, t) = C_{i,j}$, where $\underline{x} = (x,y) = (ia, ja)$. Since sites (i,j), $(i+i',j+j')$, and $(i+i'',j+j'')$ appearing in the sum in (4) are typically far-separated,

correlations between the occupancies of these sites should be negligible. Then, factorizing 3-site probabilities and converting (3) to coarse-grained continuum notation yields

$$\partial/\partial t\ C(\underline{x}, t) = -p\ C(\underline{x}, t) + K_{tot}(\underline{x}, t), \tag{5}$$

$$\text{where } K_{tot}(\underline{x}, t) \approx [1-C(\underline{x}, t)]\ [a^{-2}N^{-1} \iint_{\Omega_N} d\underline{x}'\ C(\underline{x}+\underline{x}', t)]^{2}. \tag{6}$$

It is the availability of this exact integro-differential equation (IDE) which will allow the possibility of exact analysis and elucidation of model behavior for large N.

Specifically, the IDE enables analysis of the evolution of planar interfaces with normal $\underline{n}$ separating the populated and vacuum states where $C(\underline{x}, t) = C(\underline{x}\cdot\underline{n} - V t)$ with $C \to 0$ (C_{act}), as $\underline{x}\cdot\underline{n} \to -\infty$ ($+\infty$). We will focus on LxL square neighborhoods, and circular neighborhoods of radius R. To this end, we introduce a naturally rescaled spatial variable $u \propto \underline{x}\cdot\underline{n}$, and recast (5) for planar interfaces as

$$\partial/\partial t\ C(u, t) = -pC(u, t) + [1-C(u, t)][\ \int du'K(u')\ C(u+u', t)\ ]^{2}, \tag{7}$$

where even $K(u)$ satisfies $\int du\ K(u) = \int du\ u^2\ K(u) = 1$ and $K(u) > 0$ for $-u_s < u < +u_s$. For an LxL square neighborhood, vertical interfaces correspond to $u = \sqrt{12}\ x/L$ and $K(u) = 1/\sqrt{12}$ with $u_s = \sqrt{3}$, and diagonal interfaces to $u = \sqrt{12}\ (x-y)/L$ and $K(u) = (1 - |u|/\sqrt{6})/\sqrt{6}$ with $u_s = \sqrt{6}$. For a circular neighborhood of radius R, one has that $u = 2x/R$ and $K(u) = \pi^{-1}(1- u^2/4)^{1/2}$ with $u_s = 2$. (7) has solutions of the form $C(u, t) = C(u-vt)$, but we focus on stationary interfaces ($v=V=0$) corresponding to $p=p_{eq}$. The feature that $K(u)$ depends on interface orientation and neighborhood shape suggests that the same is true of p_{eq}, i.e. that generic 2PC persists as $N\to\infty$ in the spirit of the Grinstein hypothesis [37]. Remarkably, we show that this is not the case!

It is also instructive to note that numerical analysis of (7) introduces a periodic spatial grid $u_j = ju_s/M$, and sets $C(u_j, t) = C_j(t)$. Then, a standard composite quadrature rule converts (7) into so-called lattice differential equations (LDE) [42,43]

$$d/dt\ C_j = -pC_j + (1-C_j)\ [\textstyle\sum_{-M \le m \le +M} K_m\ C_{j+m}]^{2}, \tag{8}$$

where $K_m = K(mu_s/M)/K_{sum} = K_{-m}$ for $-M < m < +M$, $K_{\pm M} = \frac{1}{2}\ K(\pm u_s)/K_{sum}$, and $K_{sum} = \frac{1}{2}K(-u_s) + \sum_{-M < m < +M} K(mu_s/M) + \frac{1}{2}K(+u_s)$. The constraint $\sum_{-M \le m \le +M} K_m = 1$ for any M ensures that (8) supports concentration profiles with the appropriate asymptotic behavior $C_j \to C_{act}(p)$, as $j \to \infty$.

To analyze stationary profile solutions, it is convenient to introduce non-analytic MF-type kinetics, $R_{MFN}(C, p) = -2[pC/(1-C)]^{1/2} + 2C$, which has the same steady-states as $R_{MF}(C, p)$ in (2). Then, the time-invariant forms of (7) and (8) at $p = p_{eq}$ become

$$\Delta^{\circ} C(u) \equiv 2 \int_{0 < u' < u_s} du'K(u')\ [C(u+u') - 2C(u) + C(u-u')] = -R_{MFN}(C(u), p_{eq}). \tag{9}$$

where $\Delta^{\circ} C(u)$ can be regarded as a non-local second derivative (reducing to $\partial^2/\partial u^2\ C(u)$ in the "diffusion approximation" [36]) and

$$\Delta_K C_j \equiv 2 \sum_{+1 \le m \le +M} K_m (C_{j+m} - 2C_j + C_{j-m}) = -R_{MFN}(C_j, p_{eq}), \quad (10)$$

where $\Delta_K C_j$ constitutes a discrete version of a second derivative. (9) and (10) also prompt consideration of stationary solutions with the appropriate asymptotics for

$$\partial^2/\partial u^2\, C(u) = -R_{MFN}(C(u), p_{eq}). \quad (11)$$

Equation (11) can be regarded as the steady-state form of a non-analytic reaction-diffusion equation (RDE). Our key point here is to emphasize the similarity in form of all of (9), (10), and (11). In all cases, p_{eq} is not known apriori.

Complete analysis of stationary profiles is non-trivial for (9) and (10). However, integrating the various types of second derivative over the profiles gives the difference of the corresponding first derivatives evaluated at $u = \pm\infty$ which vanish. Thus, we conclude that $\int_{-\infty < u < +\infty} R_{MFN}(C_{eq}(u),p_{eq})\, du = 0$ for both (9) and (11), and the analogous discrete condition applies for (10). However, (9) and (11) do not have the same stationary profile. Asymptotic analysis reveals exponential decay, $C \to C_{act}$ as u or $j \to \infty$, but the decay rate depends on the form of $K(u)$, i.e., on interface orientation and Ω_N-shape, for (9), and is different for (11). Similarly, asymptotic decay $C \to 0$ is exponential as u or $j \to -\infty$ where C and $C_j \to 0$ for (9) or (10) reveals faster than exponential decay, but one finds that $C(u) \sim p_{eq}(u-u_0)^4/36$, for $u \ge u_0$, with $C(u) \equiv 0$ for $u \le u_0$ (for finite u_0) for (11). Thus, while profiles for (9) and (11) are very similar in overall form (Fig.3a), they differ fundamentally in detail. Nonetheless, we show that (9)-(11) all share the same p_{eq}!

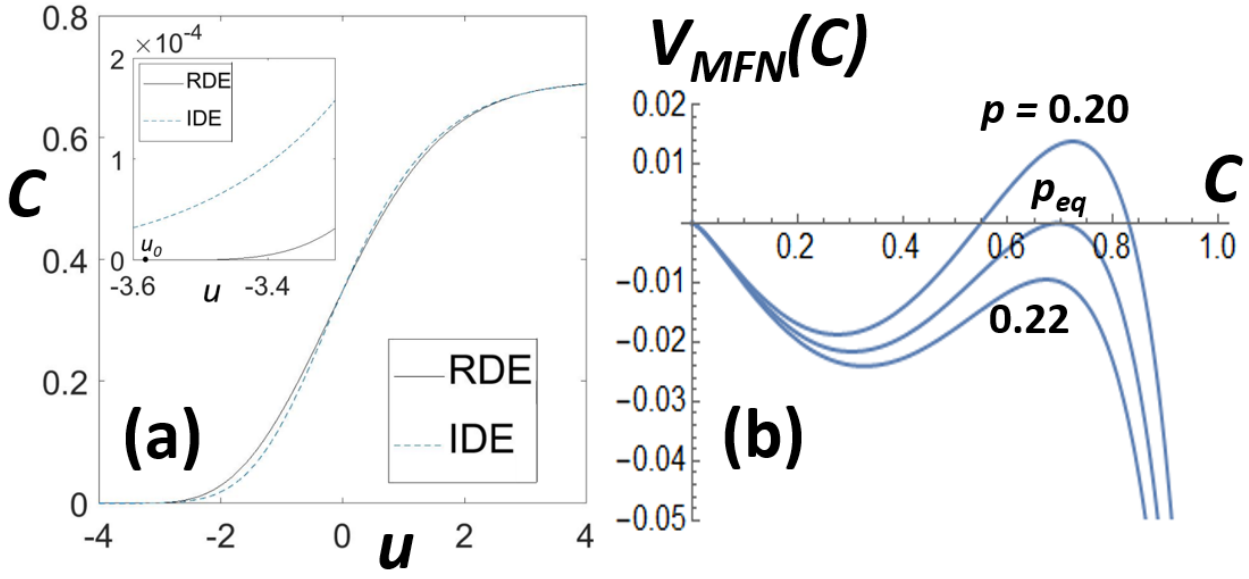

FIG. 3. (a) Stationary profiles at $p = p_{eq}$ for the IDE (9) for constant $K(u)$, and the RDE (11) where $u_0 \approx -3.5708379$. Profiles have $C(0) = C_{act}/2$. (b) $V_{MFN}(C)$ versus C from (12) for $p = 0.20$, $p = p_{eq}(MFN)$, $p = 0.22$.

Although it is not the problem of central interest, it is instructive to now provide a more complete analysis for (11) after introducing an effective potential

$$V_{MFN}(C, p) = \int_{0<C'<C} R_{MFN}(C', p)\, dC' = 2p^{1/2}[C(1-C)]^{1/2} - p^{1/2}\cos^{-1}(1-2C) + C^2, \qquad (12)$$

so that $R_{MFN}(C, p) = \partial/\partial C\, V_{MFN}(C, p)$. Fig.3b shows the form of $V_{MFN}(C, p)$. Then, (11) can be regarded as describing the motion of a pseudo-particle with position C at time u in an external potential V_{MFN}. Conservation of energy for this system implies that $E(u) = \frac{1}{2}(\partial C/\partial u)^2 + V_{MFN}(C, p)$ is u-independent. For the stationary profile at $p = p_{eq}$, the pseudo-particle starts at the potential maximum at $C = 0$ at time $u = -\infty$ with negligible velocity, and moves down the potential landscape reaching the other maximum at $C = C_{act}$ only at time $u = +\infty$. This requires equal height potential maxima (see Fig. 3b), so that $V_{MFN}(C_{act}, p_{eq}) = 0$ mimicking a Maxwell-type construction balancing positive and negative areas under $R_{MFC}(C)$ for $0 < C < C_{act}$. This relation implies that

$$(p_{eq})^{1/2}\cos^{-1}[-(1-4p_{eq})^{1/2}] = \tfrac{1}{2} + p_{eq} + \tfrac{1}{2}(1-4p_{eq})^{1/2}, \qquad (13)$$

which yields $p_{eq} = p_{eq}(MFN) = 0.2113763204128337\ldots$

Analysis of (9) and (10) is more challenging given the lack of a direct mapping onto Newtonian dynamics. However, we can embed these time-independent problems into infinite-dimensional dynamical systems incorporating Hamiltonian structure together with dissipation. All of (9)-(11) correspond to stationary solutions of dynamical equations

$$\partial^2/\partial t^2\, C = -\gamma\, \partial/\partial t\, C + \Delta^*\, C - \partial/\partial C\, \tilde{V}_{MFN}(C, p), \qquad (14)$$

where $\tilde{V}_{MFN}(C, p) = -V_{MFN}(C, p)$ is a double-well potential, $\gamma > 0$ introduces dissipation, and where $\Delta^* = \Delta^\circ$ for (9), $\Delta^* = \Delta_K$ for (10), and $\Delta^* = \partial^2/\partial u^2$ for (11).

We consider first the discrete case (10). C is replaced by C_j in the LDE (14) which constitutes a dynamical problem involving an infinite elastic chain of pseudo-particles with displacements C_j subject both to an external potential and to damping. We define total kinetic, elastic and external potential energies as

$$K = \tfrac{1}{2}\sum_{-\infty<m<+\infty}(d/dt\, C_m)^2, \quad V^{elast} = \sum_{1\le i\le+M}\sum_{-\infty<k<+\infty}\tfrac{1}{2}K_i(C_{k+1} - C_k)^2,$$

$$\text{and } V^{ext}(p) = \sum_{-\infty<m<+\infty}\tilde{V}_{MFN}(C_m, p), \qquad (15)$$

respectively. Then, it is straightforward to show that the total system energy, $E_{tot} = K + V^{elast} + V^{ext}(p)$, decreases monotonically with increasing time, t, for $\gamma > 0$.

Thus, propagating interface solutions of the LDE (14) must move in a direction corresponding to displacement of the less stable by the more stable steady state, where these correspond to higher and lower local minimum of $\tilde{V}_{MFN}$, respectively. For $p = p_{eq}(MFN)$ where the local minima of $\tilde{V}_{MFN}$ are equal, interface propagation would be inconsistent with the feature that E_{tot} should be monotonically decreasing. Thus, the LDE (14) for all $M > 1$ share the same p_{eq} as the continuum RDE [44]. Numerical analysis supports this result.

Since the LDE recover the IDE as $M\to\infty$, the IDE also have the same p_{eq}. An alternative argument notes that the IDE (14) describes the dynamics of a continuum elastic material with damping and subject to an external potential. Elastic, external, and kinetic energy functionals can be constructed generating the evolution equation (14) via functional differentiation. Then, the argument used above shows that a stationary solution only exists for $p = p_{eq}(MFN)$. In conclusion, the IDE and LDE for all interface orientations and Ω_N-shapes, and the RDE all share the same p_{eq} = 0.2113763204128337…

In summary, we explore a class of Schloegl or contact models with spontaneous particle annihilation, and autocatalytic particle creation requiring $n \geq 2$ populated sites in some neighborhood, Ω_N. Models have common MF kinetics. They exhibit a discontinuous transition between populated and vacuum states. Orientation-dependent equistability is found for small Ω_N, and might be expected for large Ω_N given the form of the governing IDEs. However, while interface profiles shape depends on orientation as $N\to\infty$, we find a unique equistability point which is shared by related LDEs and continuum non-analytic RDEs (see also [45]). We thus establish a Gibbs phase rule for these non-equilibrium models as $N\to\infty$. This elucidation of non-equilibrium phase transitions, particularly poorly understood generic 2PC behavior, is enabled by a combination of tailored KMC simulation and exact analytic treatment of spatiotemporal behavior for $N\to\infty$.

ACKNOWLEDGMENTS

DJL and JWE were supported by the USDOE BES Division of Chemical Sciences, Geosciences, and Biosciences for development of the analytic theory and the lattice-gas modeling. Research was performed at the Ames Laboratory, which is operated by Iowa State University under contract number DE-AC02-07CH11358. CJW performed the numerical analysis of evolution equations for which he was partially supported by the Ministry of Science and Technology (MOST) of Taiwan 105-2115-M-194-011-MY2.

REFERENCES

[1] J. Marro and R. Dickman, *Nonequilibrium Phase Transitions in Lattice Models* (Cambridge UP, Cambridge, 1999).
[2] G. Odor, Rev. Mod. Phys. 76, 663 (2004).
[3] M. Henkel, H. Hinrichsen, and S. Luebeck, *Non-equilibrium Phase Transitions*, Vol.1 (Springer, Berlin, 2008).
[4] H. Hinrichsen, Adv. Phys. 49, 815 (2010).
[5] *Directing Matter and Energy: Five Challenges for Science and the Imagination*, 2007 USDOE BESAC Report at http://science.energy.gov/~/media/bes/pdf/reports/files/gc_rpt.pdf.
[6] J.D. Gunton, M. San Miguel, and P.S. Sahni, in *Phase Transitions and Critical Phenomena*, edited by J.L. Lebowitz and C. Domb (Academic Press, London, 1983).
[7] R.M. Ziff, E. Gulari, and Y. Barshad, Phys. Rev. Lett. 56, 2553 (1986).
[8] J.W. Evans, D.-J. Liu, M. Tammaro, Chaos 12,131-143 (2002).
[9] A.L. Toom in *Multicomponent Random Systems*, edited by R.L. Dobrushin and Y.G. Sinai (Dekker, New York, 1980).

[10] C.H. Bennett and G. Grinstein, Phys. Rev. Lett. 55, 657 (1985).
[11] Y. He, C. Jayaprakash, and G. Grinstein, Phys. Rev. A 42, 3348 (1990).
[12] M.A. Munoz, F. de los Santos, and M.M.T. da Gama, Euro. Phys. J. B 43, 73 (2005).
[13] D.-J. Liu, X. Guo, and J.W. Evans, Phys. Rev. Lett. 98, 050601 (2007).
[14] C.-J. Wang, D.-J. Liu, and J.W. Evans, Phys. Rev. E. 142, 164105 (2015).
[15] M. Aizenman and J.L. Lebowitz, J. Phys. A: Math. Gen. 21, 3801 (1988).
[16] P.I. Hurtado, J. Marro, and P.L. Garrido, Phys. Rev. E 74, 050101R (2006)
[17] X. Guo, D.-J. Liu, and J.W. Evans, J. Chem. Phys. 130, 074106 (2009).
[18] J. Gravner, A.E. Holroyd, and R. Morris, Probab. Theory Relat. Fields 153, 1 (2012).
[19] I. Prigogine and G. Nicolis, *Self-organization in Non-Equilibrium Systems: From Dissipative Structures to Order through Fluctuations* (Wiley-Blackwell, London, 1977).
[20] A.S. Mikhailov, *Foundations of Synergetics I*: *Distributed Active Systems* 2nd Ed. (Springer Verlag, Berlin, 1994).
[21] F. Schloegl, Z. Phys. 253, 147 (1972).
[22] P. Grassberger, Z. Phys. B 47,365 (1982).
[23] A. Lawniczak, D. Dab, R. Kapral, J.-P. Boon, Physica D 47, 132 (1991).
[24] Y. De Decker, G.A. Tsekouras, A. Provata, Th. Erneux, and G. Nicolis, Phys. Rev. E 69, 036203 (2004).
[25] R. Durrett, SIAM Rev. 41, 677 (1999).
[26] S. Handjani, J. Theoret. Probab. 10, 737 (1997).
[27] L.R.G. Fontes and R.H. Schonmann, Probab. Theory Rel. Fields 141, 513 (2008).
[28] T. Montford and R.H. Schonmann, Ann. Probab. 37, 1483 (2009).
[29] S. Chatterjee and R. Durrett, Stoch. Proc. Appl. 123, 561 (2013).
[30] E.F. da Silva and M.J. de Oliveira, J. Phys. A 44, 135002 (2011).
[31] E.F. da Silva and M.J. de Oliveira, Comp. Phys. Comm. 183, 2001 (2012).
[32] M. Biskup, L. Chayes, and N. Crawford, J. Stat. Phys. 122, 1139 (2006).
[33] E. Luijten, H.W.J. Blöte, and K. Binder, Phys. Rev. E 54, 4626, (1996).
[34] C.-H. Chan and P.A. Rikvold, Phys. Rev. E 91, 012103 (2015).
[35] C.-H. Chan and P. A. Rikvold, Phys. Procedia 68, 20 (2015).
[36] D. Mollison, J. Royal Stat. Soc. Series B 39, 283 (1977).
[37] Y. He, C. Jayaprakash, and G. Grinstein, Phys. Rev. A 42, 3348 (1990).
[38] X. Guo, J.W. Evans and D.-J. Liu, Physica A 387, 177-201 (2008).
[39] C.-J. Wang, D.-J. Liu, and J.W. Evans, Phys. Rev. E. 85, 041109 (2012).
[40] R.M. Ziff and B. Brosilow, Phys. Rev. A 46, 4630 (1992).
[41] T. Tome and M.J. de Oliveira, Phys. Rev. Lett. 86, 5643 (2001).
[42] J.P. Keener, SIAM J. Appl. Math 47, 556 (1987).
[43] S.-N. Chow, J. Mallet-Paret, and E.S. Van Vleck, Int. J. Bifurc. Chaos 6, 1605 (1996).
[44] Contrasting [38,39], for $M = 1$, we find weak propagation failure anomalies which are familiar for LDE [42,43].
[45] T. Hillen, SIAM Rev. 49, 35 (2007).